Effect of cobalt precursors on the dispersion of cobalt on MCM-41

Joongjai Panpranot[a,*], Sujaree Kaewkun[a], Piyasan Praserthdam[a], and James G. Goodwin, Jr.[b]

[a]*Center of Excellence on Catalysis and Catalytic Reaction Engineering, Department of Chemical Engineering, Chulalongkorn University, Bangkok, 10330 Thailand*

[b]*Department of Chemical Engineering, Clemson University, South Carolina, 29634 USA*

Received 26 June 2003; accepted 5 September 2003

Co/MCM-41 catalysts were prepared using the incipient wetness impregnation technique with aqueous solutions of different cobalt compounds such as cobalt nitrate, cobalt chloride, cobalt acetate, and cobalt acetylacetonate. MCM-41 is known to have a restricted pore structure; however, using organic precursors such as cobalt acetate and cobalt acetylacetonate resulted in very small cobalt oxide particles that could not be detected by XRD even for a cobalt loading as high as 8 wt%. These cobalt particles were small enough to fit into the pores of MCM-41. However, they were found to chemisorb CO in only relatively small amounts and to have low activities for CO hydrogenation—probably due to the formation of cobalt silicates. The use of cobalt chloride resulted in very large cobalt particles/clusters and/or residual Cl^--blocking active sites, and, consequently, very small active surface area was measurable. The use of cobalt nitrate resulted in a number of small cobalt particles dispersed throughout MCM-41 and some larger particles located on the external surface of MCM-41. Cobalt nitrate appeared to be the best precursor for preparing high-activity MCM-41-supported cobalt Fischer–Tropsch synthesis catalysts.

KEY WORDS: cobalt catalyst preparation; cobalt precursors; MCM-41; CO hydrogenation.

1. Introduction

Co-based catalysts are widely used in CO hydrogenation or Fischer–Tropsch synthesis (FTS), especially when high molecular weight paraffins are preferred [1–3]. To increase their activity, cobalt is usually deposited on a high surface area support to obtain a high metal dispersion. The commonly used supports include silica [4–6], alumina [7–9], and titania [10,11]. Recently, attention has been focused on the use of ordered mesoporous materials such as MCM-41 as catalyst supports. MCM-41 possesses excellent support properties such as high BET surface area and well-ordered hexagonal pore structures that can be tailor-made in the pore-diameter range of 1.5–10 nm [12,13]. Their thermal and hydrothermal stability have also been improved by changing the synthesis chemicals and/or reaction conditions [14,15]. Many studies have reported significant improvements when these mesoporous materials were used as supports for catalyst preparation compared to conventional and commercial catalysts. For example, Song and Reddy [16] reported that Co-Mo supported on aluminosilicate MCM-41 prepared by impregnation showed higher hydrogenation and hydrocracking activities than conventional Co-Mo supported on γ-Al_2O_3. Schuth *et al.* [17] reported that Fe_2O_3/MCM-41 exhibited a superior performance for the conversion of SO_2 to SO_3 compared to Fe_2O_3 supported on conventional silica.

In a previous study [18], we reported the high Fischer–Tropsch activity of Ru-promoted MCM-41-supported cobalt catalysts. However, using incipient wetness impregnation with cobalt nitrate as the precursor resulted in cobalt being nonuniformly distributed on the MCM-41 support.

Besides the conventional impregnation technique, direct synthesis in which the metal ion source is introduced as a reactant into the synthesis gel and ion exchange has been widely used [19,20]. These methods, however, are limited by only small amounts of metal being able to be loaded and low metal dispersions [6]. Suvanto and coworkers reported high metal-loaded, well-dispersed Co/MCM-41 prepared using a gas-phase method and a fluidized-bed reactor [21]. This method is, however, more complicated than the conventional incipient wetness impregnation technique and may not be suitable for the preparation of commercial catalysts.

It is known that cobalt dispersion depends on the type of cobalt precursors. van de Loosdrecht *et al.* [22] showed that alumina-supported cobalt catalysts prepared by incipient wetness impregnation using cobalt EDTA and cobalt citrate precursors resulted in smaller cobalt oxide particles compared to the one prepared from cobalt nitrate. The use of cobalt oxalate, cobalt acetate, or cobalt acetylacetonate as cobalt precursors for titania-supported cobalt catalysts has been found to give higher cobalt dispersions than the catalysts prepared from cobalt nitrate [23]. Rosenek and Polansky [24] reported that use of cobalt acetate yields higher dispersion than cobalt chloride on silica. Sun *et al.* [25]

* To whom correspondence should be addressed.
E-mail: Joongjai.P@eng.chula.ac.th

1011-372X/03/1100–0095/0 © 2003 Plenum Publishing Corporation

concluded that catalysts prepared by mixed impregnation of cobalt nitrate and cobalt acetate result in higher Fischer–Tropsch synthesis activity than catalysts prepared from either monoprecursor. And recently, Soled *et al*. [26] has presented a comprehensive model for how precursor-support interactions influence the morphology and reducibility of the fresh cobalt catalysts. A balance between dispersion-enhancing strong support–precursor interaction and metal loss by retarded reduction was suggested.

However, less is known about the influence of cobalt precursors on the dispersion of cobalt when restricted pore-structure supports such as MCM-41 are used. The purpose of this study was to investigate the impact of different organic and inorganic cobalt precursors on cobalt dispersion in a restricted pore-structure support—in this case mesoporous MCM-41.

2. Experimental

2.1. Catalyst preparation

Pure silica MCM-41 was prepared in the same manner as that of Kruk *et al*. [27] using the following gel composition: $(1.0\,SiO_2) : (0.317\,TMAOH) : (0.45\,CTMABr) : (66.7\,H_2O)$, where TMAOH denotes tetramethylammonium hydroxide and CTMABr denotes cetyltrimethyl ammonium bromide. The Co/MCM-41 catalysts were prepared by the incipient wetness impregnation of the supports with aqueous solution of different cobalt precursors such as cobalt nitrate (Aldrich), cobalt acetate (APS), cobalt acetylacetonate (Aldrich) and cobalt chloride (Fluka). Cobalt loading was approximately 8% by weight of catalyst. The samples were dried at 110 °C for 1 day and were then calcined in air at 500 °C for 2 h. These catalysts with different cobalt precursors are respectively designated as Co/M-NO, Co/M-Cl, Co/M-AA, and Co/M-Ac, where Co/M refers to cobalt supported on MCM-41 and the last two letters reflect the type of the cobalt precursor used: NO for cobalt nitrate, Cl for cobalt chloride, AA for cobalt acetylacetonate, and Ac for cobalt acetate.

2.2. Catalyst characterization

2.2.1. Atomic adsorption spectroscopy

The bulk composition of cobalt was determined using a Varian Spectra A800 atomic adsorption spectrometer.

2.2.2. N_2 physisorption

The BET surface area, pore volume, average pore diameter, and pore-size distribution of the catalysts were determined by N_2 physisorption using a Micromeritics ASAP 2000 automated system. Each sample was degassed in the Micromeritics ASAP 2000 at 150 °C for 4 h prior to N_2 physisorption.

2.2.3. X-ray diffraction (XRD)

The XRD spectra of the catalysts were measured using a SIEMENS D5000 X-ray diffractometer, using Cu Kα radiation with a nickel filter in the 2–8° or 10–80 °2θ angular regions.

2.2.4. Scanning electron microscopy (SEM)

Catalyst granule morphology and elemental distribution were obtained using a JEOL JSM-35CF scanning electron microscope. The SEM was operated at 20 kV. After the SEM micrographs were taken, elemental mappings were performed to determine the elemental concentration distribution on the catalyst granules using Link Isis 300 software. The catalyst samples were cut using an ultramicrotome in order to perform SEM-EDX on different spots of cross-sectioned catalyst granules.

2.2.5. Transmission electron microscopy (TEM)

The cobalt oxide particle size and the distribution of cobalt on MCM-41 were observed using a JEOL-TEM 200CX transmission electron microscope operated at 100 kV.

2.2.6. CO-pulse experiment

Relative percentages of cobalt dispersion were determined by pulsing carbon monoxide over the reduced catalyst. Approximately 0.2 g of catalyst was placed in a quartz tube, incorporated in a temperature-controlled oven and connected to a thermal conductivity detector (TCD). Prior to chemisorption, the catalyst was reduced in a flow of hydrogen (50 cc/min) at 400 °C for 2 h. Afterward, the sample was purged with helium at 400 °C for 1 h and finally cooled down to room temperature. Carbon monoxide was pulsed at 25 °C over the reduced catalyst until the TCD signal was constant.

2.2.7. Reaction test

CO hydrogenation was carried out at 220 °C and 1 atm total pressure in a fixed-bed stainless steel reactor under differential conversion conditions. A flow rate of $H_2/CO/Ar = 20/2/8\,cm^3/min$ was used. Typically, 0.2 g of the catalyst samples was reduced *in situ* in flowing H_2 (50 cc/min) at 350 °C for 10 h prior to the reaction. The product samples were taken at 1-h intervals and analyzed by gas chromatography. Steady state was reached after 6 h time onstream in all cases.

3. Results and discussion

To determine a suitable temperature for calcination of all cobalt precursors, thermogravimetric analysis (TGA) experiments were performed with bulk cobalt nitrate, cobalt acetate, cobalt acetyl acetonate, and cobalt chloride (figure 1). All cobalt precursors appeared to be fully decomposed for calcination

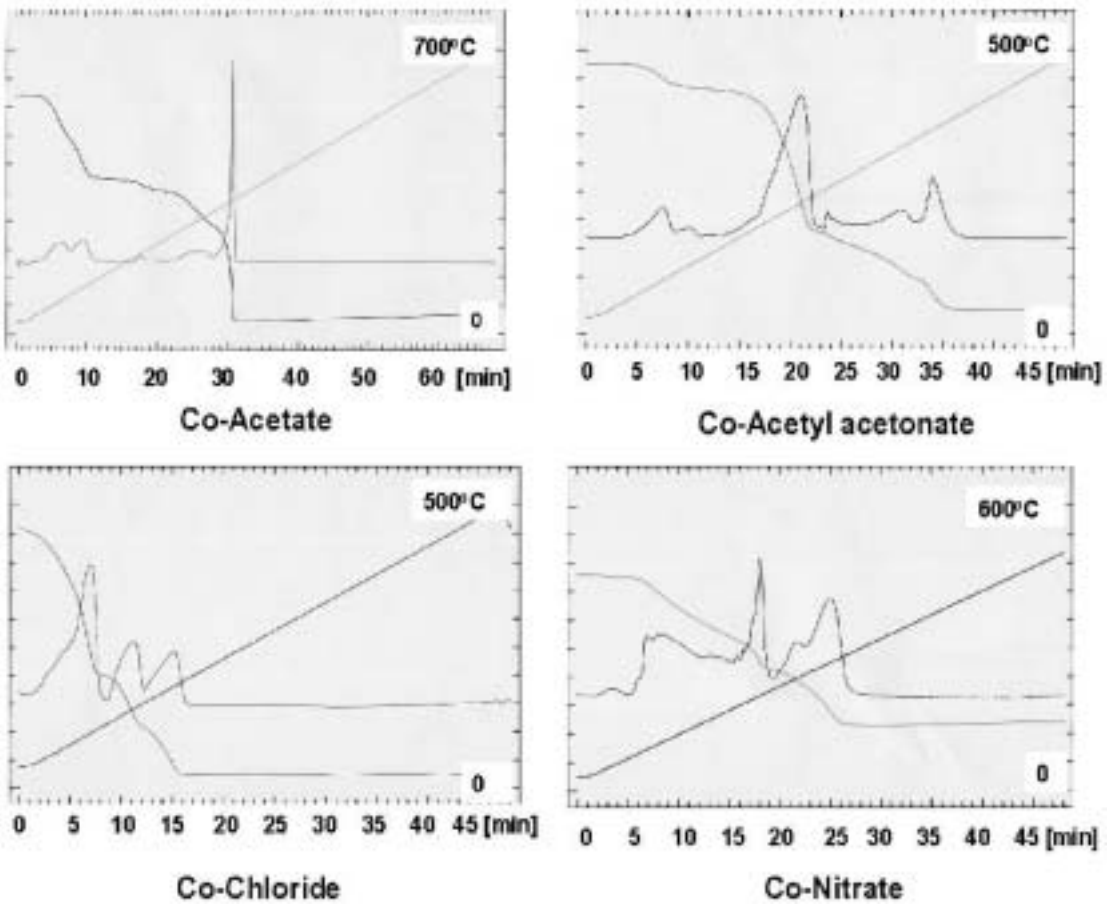

Figure 1. Thermogravimetric analysis (TGA) experiments for different cobalt precursors (bulk).

temperatures above 400 °C. Thus, a calcination procedure using 500 °C for 2 h was used to produce the cobalt oxide phase in all the various catalysts prepared.

The actual amounts of cobalt loading (determined by atomic adsorption spectroscopy), the BET surface areas, and the cobalt crystallite sizes (derived from XRD line broadening) for the catalyst samples are given in table 1. In this study, cobalt loading on the catalyst samples was approximately 7–8 wt% in order to make it close to that required for a commercial catalyst. The pure silica MCM-41 support before cobalt impregnation had a BET surface area of 1234 m^2/g and a pore volume of 0.85 cm^3/g. The BET surface areas of the cobalt catalysts prepared with different cobalt precursors were found to be in the range of 646–756 m^2/g and in the order of Co/M-Ac > Co/M-NO > Co/M-AA > Co/M-Cl. The significant decrease in surface area of the original support material suggests that cobalt was deposited significantly in the pores of MCM-41. The cobalt precursor did not have a significant impact on the average pore diameter of MCM-41 after cobalt loading since all the catalyst samples retained narrow pore-size distributions of approximately 3 nm, the same as the original MCM-41.

Table 1
Characteristics of Co/MCM-41 catalysts prepared from different cobalt precursors

Catalyst	Co[a] (wt%)	BET S.A.[b] (m^2/g)	dp[c] Co_3O_4 (nm)
MCM-41	—	1234	—
Co/M-Ac	8.3	756	<5
Co/M-AA	7.8	675	<5
Co/M-Cl	7.1	646	15.0
Co/M-NO	8.1	747	6.3

[a]Elemental analysis using atomic adsorption spectroscopy. Error of measurement = ±2%.
[b]Using N_2 physisorption at 77 K. Error of measurement = ±10%.
[c]From XRD line broadening. Error of measurement = ±5%.

The XRD patterns of the MCM-41-supported cobalt catalysts are shown in figure 2. The ordered structure of MCM-41 gave an XRD peak at low 2θ around 2.58° for the unsupported MCM-41. After impregnation of cobalt, the intensity of the XRD peaks for MCM-41 was decreased for all the catalyst samples and the peaks became broader owing to the structure of MCM-41 becoming less ordered by the impregnation of cobalt or because of the secondary scattering of the X rays. The structure of MCM-41 was not destroyed, but the long-range order of MCM-41 may have shrunk [28].

The XRD patterns at higher diffraction angles of the MCM-41-supported cobalt catalysts prepared with

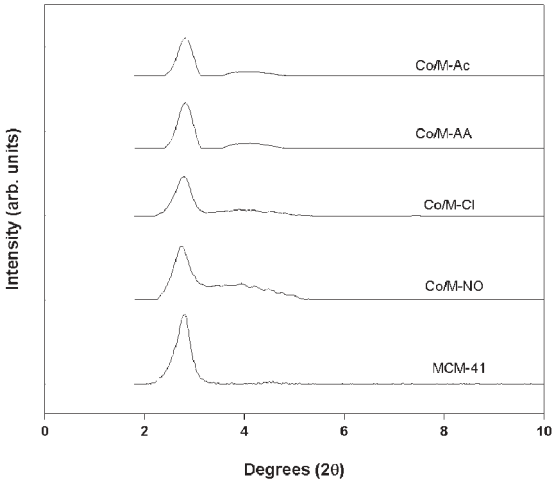

Figure 2. Effect of cobalt precursors on the XRD patterns of Co/MCM-41 catalysts (low 2θ).

different cobalt precursors in the calcined state are shown in figure 3. Co/M-NO and Co/M-Cl exhibited diffraction peaks at 2θ of ca. 31.3°, 36.8°, 45.1°, 59.4°, and 65.4°, indicating the presence of Co_3O_4 spinel in the catalyst particles. Surprisingly, Co/M-Ac and Co/M-AA did not exhibit any distinct XRD patterns. This suggests that the crystallite size of cobalt oxide prepared from cobalt acetate and cobalt acetylacetonate on MCM-41 was below the lower limit for XRD detectability (5 nm) even though cobalt loading was as high as 8 wt%. It is also possible that on Co/M-Ac and Co/M-AA, cobalt did not form Co_3O_4 crystallites but may have formed an amorphous cobalt oxide similar to what has been suggested for Co/TiO_2 prepared from cobalt EDTA [23]. For Co/M-NO and Co/M-Cl, the average cobalt oxide crystallite sizes calculated using the Scherrer's equation [29] were found to be 6.3 and 15.0 nm, respectively. These cobalt particles were much larger than the average pore diameter of MCM-41 (3 nm), suggesting that using cobalt nitrate and cobalt chloride precursors to prepare MCM-41-supported cobalt catalysts by incipient wetness impregnation resulted in some large cobalt oxide particles deposited on the external surface of MCM-41.

SEM and elemental mapping were carried out for all the catalyst samples. Typical SEM micrographs of catalyst granules are shown in figure 4. The term "granule" here refers to a catalyst particle composed of cobalt and silica. In all the SEM figures, the white or light spots on the catalyst granules represent a high concentration of cobalt and its compounds, while the darker areas of the granules indicate the support with minimal/no cobalt present. The dark background is due to the carbon tape used for holding the catalyst samples. The SEM micrographs for catalyst granules prepared with different cobalt precursors show similar catalyst granule sizes of 30–50 μm. The elemental mappings for cobalt are shown in figure 5. The presence of very large cobalt clusters nonuniformly distributed on the granule exteriors was observed for Co/M-Cl. Dispersion of the cobalt was better for the other catalysts.

SEM-EDX was performed on cross-sectioned catalyst granules in order to determine the cobalt concentration at different locations on the catalyst granules (in the pores versus on the external surface). The SEM

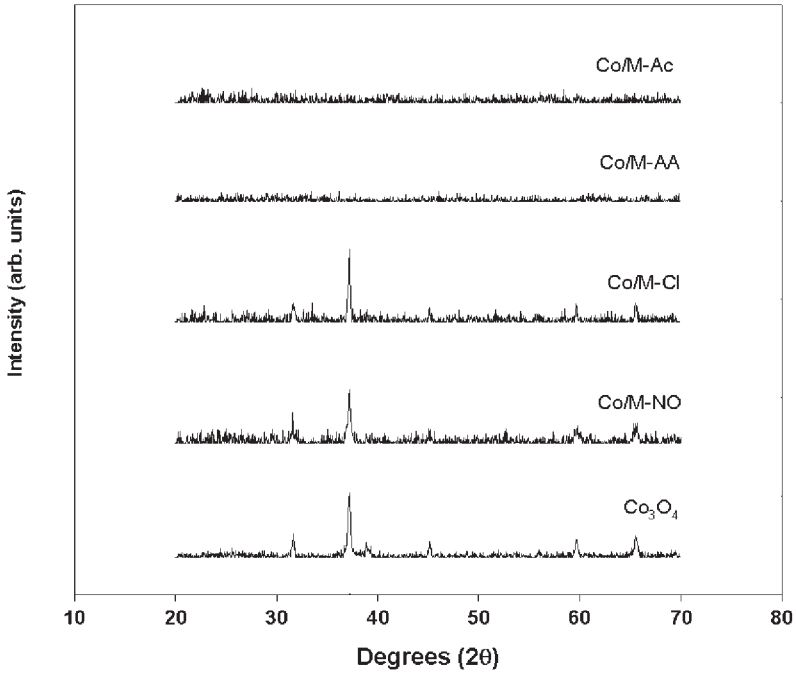

Figure 3. Effect of cobalt precursors on the XRD patterns of Co/MCM-41 catalysts (high 2θ).

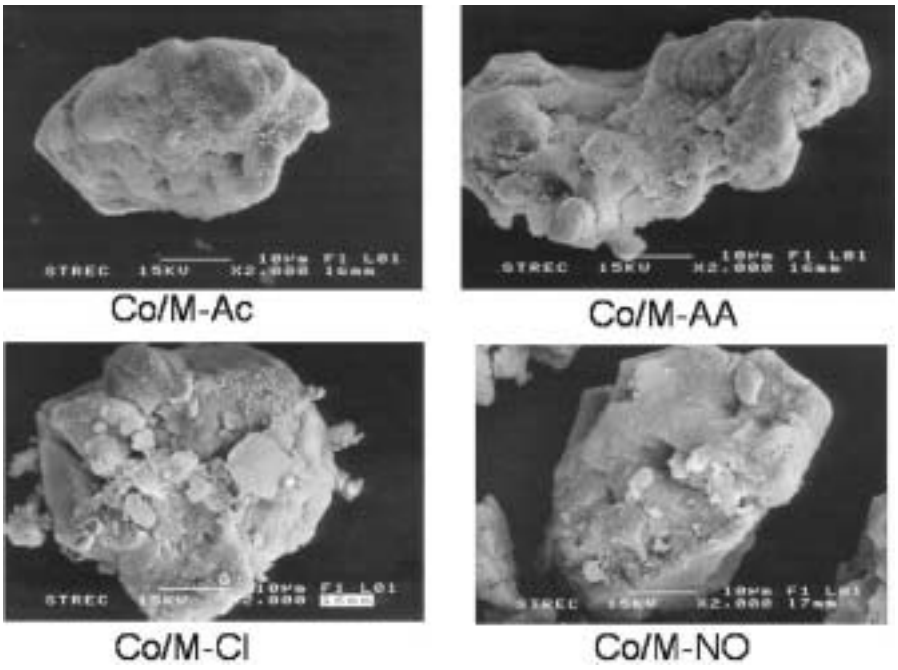

Figure 4. SEM micrographs of Co/MCM-41 catalysts prepared with different cobalt precursors.

micrographs of cross-sectioned catalyst granules with locations of EDX analysis are shown in figure 6. The corresponding elemental distributions are reported in table 2. Again, we observed a very high concentration of cobalt on the external surface of Co/M-Cl, whereas distribution of cobalt for the other catalysts was not significantly different across the cross-sectioned granules. SEM-EDX results thus confirm that, except for

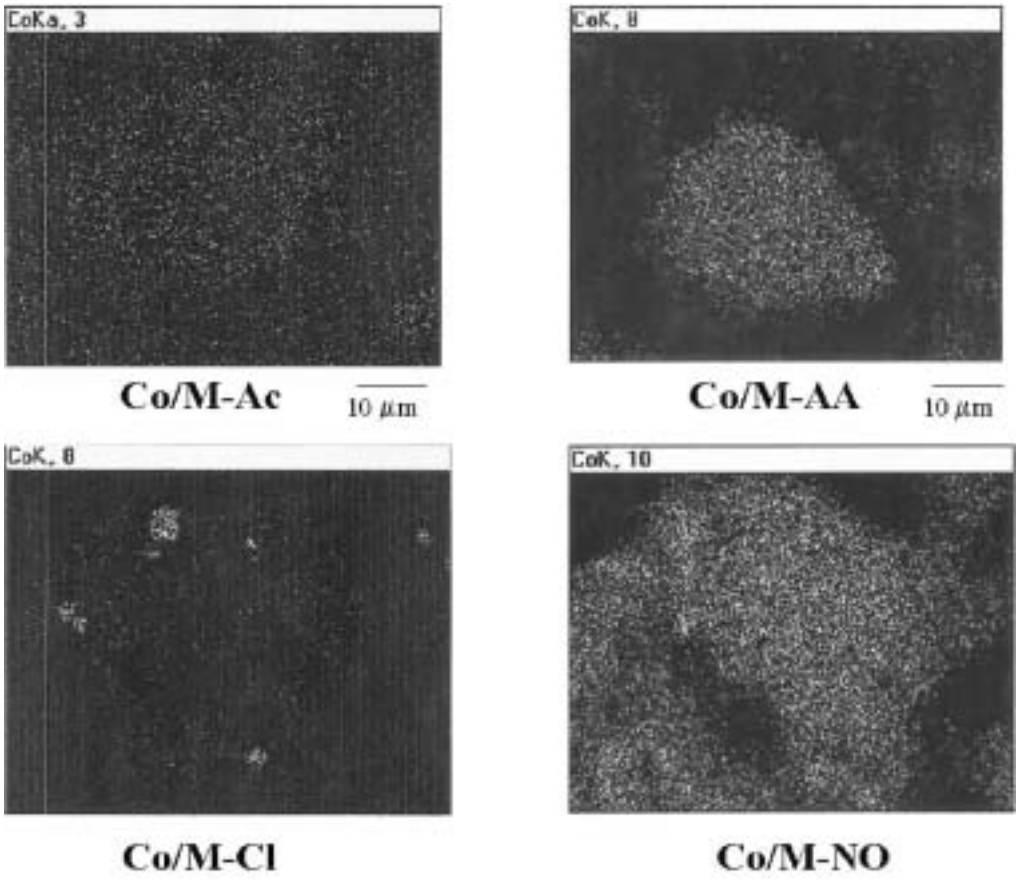

Figure 5. Distribution of cobalt on the exteriors of different Co/MCM-41 catalyst granules from SEM elemental mappings.

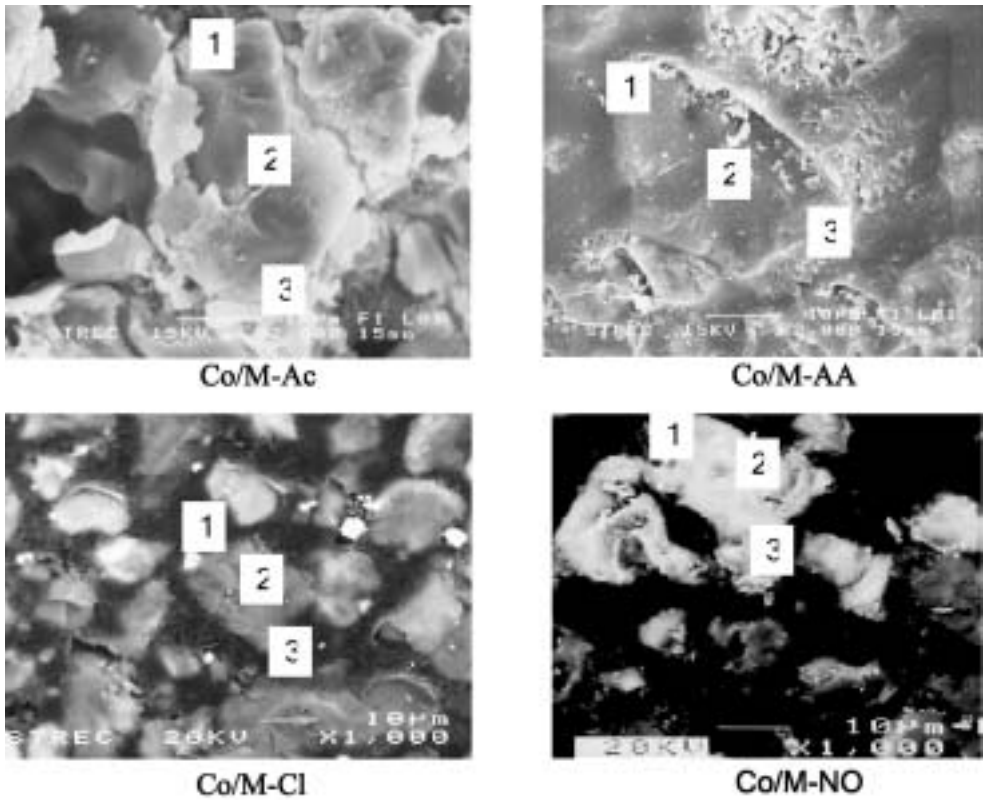

Figure 6. SEM micrograph of the cross-sectioned catalysts with locations of EDX analysis.

Co/M-Cl, the cobalt catalysts had their cobalt primarily located in the pores of MCM-41.

TEM micrographs were taken for all the catalysts in order to physically measure the size of cobalt oxide particles and/or cobalt clusters (figure 7). TEM images were found to be in accordance with the results from XRD and EDX that very large cobalt clusters (1–2 μm) were present on Co/M-Cl, while dispersion of the cobalt was better for the other catalysts. Although TEM measurements were only done for a very small portion of each catalyst, the results are able to provide further evidence about cobalt dispersion.

The degrees of reduction, the relative rankings of cobalt dispersion, and the CO hydrogenation rates of the catalysts are reported in table 3. The degrees of reduction of the catalysts in the TGA experiments from 30–800 °C were not significantly different, ranging from 53–64%, with Co/M-NO showing the highest degree of reduction. Any cobalt not reducible during the H_2 reduction up to 800 °C is identified as ''nonreducible'' cobalt silicate [30,31].

Table 2
Elemental analysis using SEM-EDX on different locations of the cross-sectioned catalysts

Catalyst	Co (wt%)[a]		
	Location 1	Location 2	Location 3
Co/M-Ac	7.5	10.6	7.8
Co/M-AA	11.4	12.4	6.5
Co/M-Cl	18.6	4.9	6.9
Co/M-NO	7.9	6.0	7.7

[a]Error of measurement = ±10%.

The relative ranking of cobalt dispersion was calculated from CO-pulse chemisorption experiments. Since for CO chemisorption on cobalt, bridge bonding may occur, there is no precise ratio of CO molecules to cobalt metal surface atoms that can be used. However, for strictly identical measurement conditions, CO chemisorption can yield a relative ranking of cobalt dispersion. It was found that CO chemisorption was only measurable for Co/M-AA and Co/M-NO, with Co/M-AA exhibiting higher amount of CO chemisorption than Co/M-NO. Co/M-Cl exhibited negligible chemisorption probably due to its low dispersion of cobalt and/or due to residual Cl^- blocking the cobalt sites. Residual Cl^- has been found in other supported metal catalysts when Cl-containing compounds are used as the catalyst precursor [32–34]. Figure 8 shows the XRD pattern of bulk $CoCl_2$ after calcination at 500 °C, where residual Cl^- can be observed. However, residual Cl^- was probably highly dispersed or present in very low amounts so that it could not be detected by XRD in case of the Co/M-Cl catalyst. One should note that residual Cl^- has been shown to be significantly decreased in metal catalysts when water vapor is

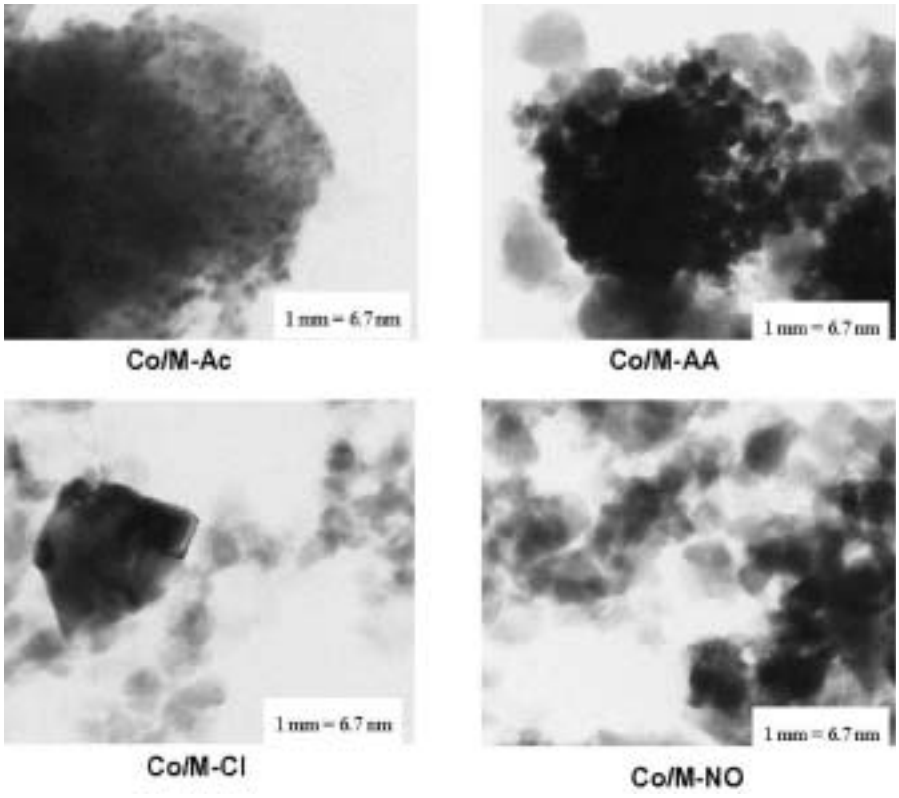

Figure 7. TEM micrographs of Co/MCM-41 catalysts prepared with different cobalt precursors.

present, such as during CO hydrogenation. Co/M-Ac had well-dispersed cobalt as determined by XRD and TEM; therefore, it is surprising that no CO adsorption could be measured at the conditions used.

The test reactions for CO hydrogenation were carried out at 220 °C, 1 atm, and H_2/CO ratio = 10 for all catalyst samples. A relatively high H_2/CO ratio was used in order to minimize deactivation due to carbon deposition during reaction. It was found that at the reaction conditions used, Co/M-NO exhibited a much higher CO hydrogenation rate than all other catalysts in this study. The low activity of Co/M-Ac and Co/M-AA is probably due to the unstable small cobalt particles forming cobalt silicates during reduction in H_2 [31,35] due to the water vapor generated.

The results of this study were found to be in agreement with the well-established trends in the literature on the influence of cobalt precursors on different supported cobalt Fischer–Tropsch catalysts [22–26]. It should be emphasized that our results support the need for a balance between dispersion-enhancing, strong support-precursor interaction and loss of metallic cobalt as a result of metal-support compound formation in order to obtain high-activity-supported cobalt catalysts, in agreement with the recent suggestions of Soled *et al.* [26]. The type of cobalt precursor must be carefully chosen, especially when restricted pore-structure supports such as MCM-41 are used. Cobalt particles small enough to fit into the pores of MCM-41 could be unstable at commercially relevant

Table 3
Results from TGA, CO-pulse chemisorption, and CO hydrogenation reaction

Catalyst	Reducibility[a] (30–800 °C)	CO chemisorption $(CO/Co)^b \times 100$	Rate[c] $\times 10^4$ ($g_{CH_2}/g_{cat.}/h$)	
			Initial	Steady state
Co/M-Ac	59	Nil	0.068	0.057
Co/M-AA	53	7.6	0.338	0.071
Co/M-Cl	58	Nil	0.012	0.050
Co/M-NO	64	2.6	1.810	1.150

[a]From thermogravimetric experiments.
[b]The relative %Co dispersion from pulse CO chemisorption experiments.
[c]CO hydrogenation was carried out at 220 °C, 1 atm, $H_2/CO = 10$ ($H_2/CO/Ar = 20/2/8$ cc/min).

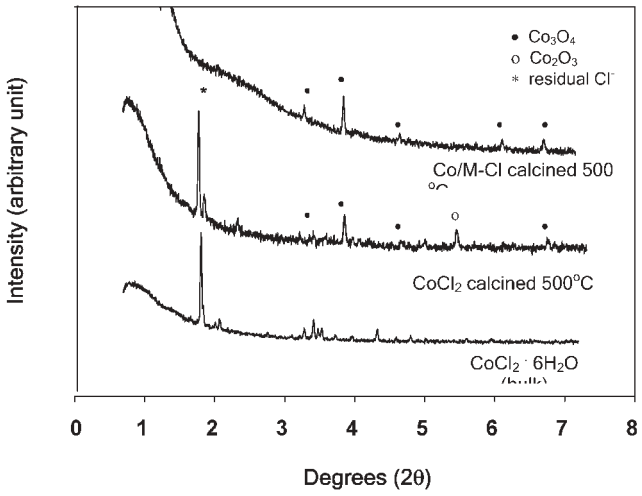

Figure 8. XRD pattern of residual Cl^- after calcination at 500 °C for 2 h.

synthesis conditions and thus have limited practical use.

4. Conclusion

Using organic precursors such as cobalt acetate or cobalt acetylacetonate instead of inorganic ones such as cobalt nitrate or cobalt chloride results in very small cobalt particles uniformly distributed throughout the pore structure of MCM-41. Extremely large cobalt particles/clusters are evident on Co/MCM-41 prepared from cobalt chloride. The results suggest, however, that there may be an optimum cobalt particle size and dispersion to maximize the surface cobalt availability since cobalt silicate formation during reduction may occur (especially for highly dispersed cobalt) and result in lower CO hydrogenation activity. Only surface cobalt metal atoms are active for CO hydrogenation. Among the four types of cobalt compounds used in this study, cobalt nitrate seems to be the best (optimum) cobalt precursor to prepare MCM-41-supported cobalt catalysts with significant CO hydrogenation activity at commercially relevant synthesis conditions.

Acknowledgment

Financial support by the Thailand Research Fund (TRF) and TJTTP-JBIC is gratefully acknowledged.

References

[1] R.B. Anderson, *The Fischer–Tropsch Synthesis* (Academic Press, San Diego, 1984).
[2] J.G. Goodwin Jr., Prep. ACS Div. Petr. Chem. 36 (1991) 156.
[3] E. Iglesia, Appl. Catal. A 161 (1997) 50.
[4] R.C. Reuel and C.H. Bartholomew, J. Catal. 85 (1984) 78.
[5] L.B. Backman, A. Rautiainen, A.O.I. Krause and M. Lindblad, Catal. Today 43 (1998) 11.
[6] G.J. Haddad and J.G. Goodwin Jr., J. Catal. 157 (1995) 25.
[7] J. van de Loosdrecht, M. van der Haar, A.M. van der Krann and J.W. Geus, Appl. Catal. A 150 (1997) 365.
[8] A.R. Belambe, R. Oukaci and J.G. Goodwin Jr., J. Catal. 166 (1997) 8.
[9] D. Schanke, A.M. Hilmen, E. Bergene, K. Kinnari, E. Rytten, E. Adnanes and A. Holmen, Catal. Lett. 34 (1995) 269.
[10] J.H.A. Martens, H.F.J. van't Blik and R. Prins, J. Catal. 97 (1986) 200.
[11] J. Li and N.J. Coville, Appl. Catal. A 181 (1999) 201.
[12] J.S. Beck, J.C. Vartuli, W.J. Roth, M.E. Leonowicz, C.T. Kresge, K.D. Schmitt, C.T.-W. Chu, D.H. Olson, E.W. Sheppard, S.B. McCullen, J.B. Higgins and J.L. Schlenker, J. Am. Chem. Soc. 114 (1992) 10834.
[13] C.T. Kresge, M.E. Leonowicz, W.J. Roth, J.C. Vartuli and J.S. Beck, Nature 359 (1992) 710.
[14] E. Zhao, J. Feng, Q. Huo, N. Melosh, G.H. Fredrickson, B.F. Chmelka and G.D. Stucky, Science 279 (1998) 548.
[15] E. Zhao, Q. Huo, J. Feng, B.F. Chmelka and G.D. Stucky, J. Am. Chem. Soc. 120 (1998) 6024.
[16] C. Song and K.M. Reddy, Appl. Catal. A 176 (1999) 1.
[17] F. Schuth, A. Wingen and J. Sauer, Microporous and Mesoporous Mater. 44–45 (2001) 465.
[18] J. Panpranot, J.G. Goodwin Jr. and A. Sayari, J. Catal. 211 (2002) 530.
[19] A. Jentys, N.H. Pham, H. Vinek, M. Englisch and J.A. Lercher, Microporous Mater. 6 (1996) 13.
[20] A. Jentys, N.H. Pham, H. Vinek, M. Englisch and J.A. Lercher, Catal. Today 39 (1998) 311.
[21] S. Suvanto, J. Hukkamaki, T.T. Pakkanen and T.A. Pakkanen, Langmuir 16 (2000) 4109.
[22] J. van der Loosdrecht, M. van der Haar, A.M. van der Kraan, A.J. van Dillen and J.W. Geus, Appl. Catal. A 150 (1997) 365.
[23] M. Kraum and M. Baerns, Appl. Catal. 186 (1999) 189.
[24] M.P. Rosynek and C.A. Polansky, Appl. Catal. 73 (1991) 97.
[25] S. Sun, N. Tsubaki and K. Fujimoto, Appl. Catal. A 202 (2000) 121.
[26] S.L. Soled, E. Iglesia, R.A. Fiato, J.E. Baumgartner, H.B. Vroman and S. Miseo, Paper 293, *18th North American Catalysis Society Meeting*, Cancun, Mexico, 1–6 June 2003.
[27] M. Kruk, M. Jaronice and A. Sayari, Microporous Mesoporous Mater. 35–36 (2000) 545.
[28] L. Pasqua, F. Testa, R. Aiello, F. Di Renzo and F. Fajula, Microporous and Mesoporous Mater. 44–45 (2001) 111.
[29] H.P. Klug and L.E. Alexander, *X-ray Diffraction Procedures for Polycrystalline Amorphous Materials*, 2nd ed. (Wiley, New York, 1974).
[30] L.B. Backman, A. Rautiainen, A.O.I. Krause and M. Lindblad, Catal. Today 43 (1998) 11.
[31] A. Kogelbauer, J.C. Webber and J.G. Goodwin Jr., Catal. Lett. 34 (1995) 259.
[32] N. Mahata and V. Vishwanathan, J. Catal. 196 (2000) 262.
[33] Y. Zhou, M.C. Wood and N. Winograd, J. Catal. 146 (1994) 82.
[34] P. Johnston and R.W. Joyner, J. Chem. Soc. Faraday Trans. 89 (1993) 863.
[35] J.M. Jablonski, M. Wolcyrz and L. Krajczyk, J. Catal. 173 (1998) 530.